Available online at www.sciencedirect.com
SCIENCE DIRECT®

Journal of the European Ceramic Society 23 (2003) 3079–3087
www.elsevier.com/locate/jeurceramsoc

Effect of the particle size distribution of spinel on the mechanical properties and thermal shock performance of MgO–spinel composites

Cemail Aksel[a,*], Frank L. Riley[b]

[a]Department of Materials Science and Engineering, Anadolu University, Iki Eylül Campus, Eskisehir 26470, Turkey
[b]Department of Materials, School of Process, Environmental and Materials Engineering, University of Leeds, Leeds LS2 9JT, UK

Received 24 August 2002; received in revised form 16 January 2003; accepted 1 February 2003

Abstract

The influence of varying the amounts of spinel with a similar median particle size, but with different distribution, on the mechanical properties and thermal shock performance of MgO–spinel composites was investigated. Mechanical properties of composites decreased significantly with increasing spinel content due to the thermal expansion mismatch. However, γ_{WOF} values of composites increased markedly, because of a significant change in the fracture mode from transgranular to intergranular fracture. A narrow distributed spinel A (Alcoa MR66) particles resulted in shorter initial crack propagation distances from the spinel particles, but spinel B (Britmag 67) particles with a significantly broader distribution were the origins of longer interlinked cracks. The improved resistance to thermal shock in MgO–spinel composites can therefore be attributed to the microcrack networks developed around the spinel particles, associated with the high values of γ_{WOF}, and not to an increased K_{1c}. On the basis of theoretically calculated R''' values and experimentally found γ_{WOF}/γ_i ratios, resistance to thermal shock damage would be more strongly favoured with materials containing spinel B particles, rather than spinel A, for which a much larger volume% was required to achieve a similar improvement.

Keywords: Fracture surface energy; Mechanical properties; $MgAl_2O_4$; MgO; Particle size distribution; Thermal shock resistance; Work of fracture

1. Introduction

The spinels are a class of double oxide of general formula AB_2O_4: industrially important members of this class include aluminates (e.g. $MgAl_2O_4$), ferrites (e.g. $MgFe_2O_4$) and chromites (e.g. $MgCr_2O_4$). Chrome ore consists primarily of the mineral Chromite, which is a mixture of spinels represented by the general formula $(Mg,Fe)O.(Cr,Al,Fe)_2O_3$.[1,2] Chrome was first used on a large scale as a neutral steel plant refractory more than 100 years ago, and its use became widespread because of its good resistance to spalling (the abrupt loss of hot face material).[3] Chrome–magnesite refractories, mixtures of chrome ore and magnesite containing 20 to 80% chrome, were developed extensively in the early 1930's because of their high strength at high temperatures, and their much better thermal shock resistance than refractories based on chrome alone. The magnesite–chrome and chrome–magnesite ranges of refractory material were subsequently intensively used for applications requiring a high hot-strength and resistance to attack by basic slags and molten metals.[4] An important example of this type of environment is the rotary cement kiln lining, with centre zone temperatures exceeding 1600 °C, and the presence of semi-liquid and corrosive calcium aluminosilicates.

Increasing concern over the toxicity of the Cr(VI) produced from Cr_2O_3 under alkaline conditions has meant that the handling and disposal of waste refractories containing chrome are now being subject to strict European Union regulations,[5] and alternative refractory materials which do not contain Cr_2O_3 are needed. Magnesite and dolomite refractories are satisfactory in many respects for the types of application previously

* Corresponding author. Tel.: +90-222-335-0580x6355; fax: +90-222-323-9501.
E-mail address: caksel@anadolu.edu.tr (C. Aksel).

0955-2219/03/$ - see front matter © 2003 Elsevier Ltd. All rights reserved.
doi:10.1016/S0955-2219(03)00102-X

using magnesite–chrome materials, but lack their good resistance to thermal shock. It has been found that this deficiency can be overcome by incorporating into a magnesite matrix 9–30% of particulate magnesium aluminate spinel ($MgAl_2O_4$), to form the magnesia–spinel materials.[6,7] Magnesia–spinel refractories were first evaluated more than 30 years ago,[4] but it has only been during the last decade that marked efforts have been made to use them as alternative refractories to magnesia–chrome materials. Fortuitously, magnesia–spinel refractories also have the additional important advantage of a longer (1.5–2 times) life than an otherwise equivalent magnesite–chrome refractory, particularly in locations where they are exposed to high temperatures and severe thermal shock.[8]

The reasons for the improved performance of the magnesia–spinel composites have been very loosely ascribed to an improved "elasticity" or "toughness".[9,10] The current consensus of opinion is that[11,12] the fundamental reason is primarily the large difference in thermal expansion coefficient between MgO (13.6×10^{-6} $^{\circ}C^{-1}$ from 25 °C to 1000 °C) and spinel (8.4×10^{-6} $^{\circ}C^{-1}$ from 25 °C to 1000 °C).[13,14] During cooling from production temperatures in the region of 1650 °C the difference generates very large hoop tensile stresses around the spinel particles, causing extensive microcracking.[9] The microcracks decrease the overall strength and stiffness, but they may also either be barriers to subsequent crack propagation in service, or allow stress relief during heating. The improved resistance to thermal shock in MgO–spinel composites can therefore be attributed to the microcrack networks developed around the spinel particles.[11,12,15]

The general basic principles relating microstructure to thermomechanical properties in ceramic–ceramic matrix composites, of which the magnesia–spinel refractories are an example, are well established.[16] However there remain uncertainties with regard to important points of fine detail, and to specific systems. It is difficult, for example, to predict the critical particle size required to initiate spontaneous microcracking in these composites.[17] Problems of interpretation in the magnesia–spinel case are also created by a tendency to nonlinear elastic behaviour,[18] which it has been suggested is caused by the relief of stress by microcrack propagation during loading.

Numerous (almost all industrially based) studies have been made over the last 15 years, with the objective of developing magnesia–spinel materials of improved resistance to thermal shock and alkali attack. The work done so far has been mainly phenomenological, and little quantitative understanding of the function of the system variables has been developed. It is therefore still difficult to specify optimum compositions with confidence, and materials development is based largely on trial and error. Much of the magnesia–spinel refractory currently produced is used for cement kiln linings, where there are two conflicting requirements: for thermal shock resistance the optimum spinel content should be fairly high; for reduced calcium oxide attack, involving reaction with aluminium oxide (Al_2O_3) and the formation of low melting calcium aluminates, the spinel content must be as low as possible. It is clearly necessary to keep the spinel content to a minimum, while developing the maximum resistance to thermal shock.[19] The optimum spinel content has been claimed to be as high as ~40% by previous researchers.[9] Subsequent researchers have used a range of model, high purity, magnesia–spinel composites to examine in detail the effects of spinel particle size and quantity on thermomechanical behaviour, and suggested an optimum composite composition for a maximum resistance to further damage by thermal shock of ~20% of spinel.[12,20] In spite of the importance of this refractory system, few fundamental underpinning scientific studies have been reported so far, apart from the most recent researchers.[11,12,15,20–22] It seems that understanding of the influence of the particle size distribution on thermomechanical behaviour is also rudimentary.

It has been reported that microcracking caused by the addition of spinel reduces both strength and stiffness, and fracture toughness (K_{1c}) always decreases with spinel additions.[11,21,22] The R''' parameter expresses the ability of a material to resist crack propagation and further damage and loss of strength on thermal shocking. The trends in the R''' parameter are consistent with measurements of thermal shock damage caused by quenching, providing quantitative confirmation of the view that the extent of microcrack propagation and interlinking controlled by spinel particle size and volume, is important for thermomechanical behaviour.[12,20] This work aims to quantify the influence of these parameters on mechanical property and on consequent thermal shock behaviour by using a similar median particle size, but with different distribution of spinel, on the basis of the changes in R''' values and γ_{WOF}/γ_i ratios. It is expected that this study will provide a platform for extended work for detailed modelling of the thermal shock behaviour and high temperature properties of magnesia–spinel composite materials, and develop guidelines to allow the optimisation of commercial magnesia–spinel refractory compositions and microstructures.

2. Experimental

In this present work, calcined MgO and two types of spinel powders were used: 22 and 24 μm spinel. Particle size distributions for all powders were determined using a laser light scattering particle sizer (Malvern Mastersizer/E, UK), and specific surface areas $\{A_s = 6/(\rho D_p)\}$

were determined using a single point nitrogen adsorption technique (Perkin-Elmer Ltd., 212D Sorptometer, Beaconsfield, UK), where ρ is the true solid density and D_p is the particle equivalent diameter. To improve densification behaviour, a nano-particle size MgO powder ('light': GPR, BDH, Poole, UK) was calcined at 1300 °C for 2 h, which yielded a powder of mean particle size ~0.5 μm. Two types of preformed spinel powder were then incorporated into calcined MgO: i) Alcoa MR66 spinel powder (Alcoa International Ltd., UK), defined as 'A', was air classified to obtain more narrow distributions of median size 22 μm, and ii) Britmag 67 spinel powder, defined as 'B', of median particle size 24 μm was obtained by crushing ('Shatter Box', Glen Creston Ltd., UK) and by using a 150 μm sieve, high density spinel 'pebbles' (Britmag 67, Lafarge, UK). 22 μm spinel powder had higher purity than 24 μm spinel powder. The amounts of impurities in the powders as wt.% were i) 0.15% Cl, 0.50% SO_4, 0.05% Fe for MgO, ii) 0.23% CaO, 0.13% Fe_2O_3, 0.01% MnO, 0.01% TiO_2, 0.01% Na_2O, 0.01% P_2O_5 for Alcoa MR66 spinel, and iii) 0.74% CaO, 0.68% SiO_2, 0.64% Fe_2O_3, 0.02% MnO, 0.01% TiO_2, 0.01% K_2O for Britmag 67 spinel. The spinel stoichiometry is given by wt.% as follows: i) 66.3% Al_2O_3 and 33.3% MgO for Alcoa MR66 spinel, and ii) 66.3% Al_2O_3 and 31.6% MgO for Britmag 67 spinel. The effects of varying the amounts (5, 10, 20 and 30 wt.%) of spinel with a similar median particle sizes, but with different particle size distribution and purities, were investigated. The MgO–spinel composites, containing 0–30 wt.% spinel, could be obtained theoretically dense (~99%), by hot-pressing at 1720 °C and 20 MPa for 25 min. Bulk density and apparent porosity were measured using the standard water immersion method.[23] The room temperature strength of the hot-pressed pure MgO using three-point bend test was in good agreement with the literature values,[24,25] and thus mechanical measurements of all the spinel composites were made in three-point bend, with a support roller span of 20 mm and a cross-head speed of 0.2 mm min^{-1}. Five specimens were normally tested to obtain a mean value, using a tensile testing machine (Mayes, SMT50). The standard equations for the strength (σ_f)[26] and Young's Modulus (E)[27] of a bar (Pa) in three-point bend are:

$$\sigma_f = (3/2).(PL)/(WD^2) \quad (1)$$

$$E = L^3.m/(4WD^3) \quad (2)$$

where P = load at fracture, L = support span, W = specimen width, and D = specimen thickness, m = slope of the tangent of the initial straight-line portion of the load–deflection curve. Modulus values were calculated by drawing a tangent to the steepest initial straight-line portion of the load–deflection curve, (the stiffness of the machine was also considered), using Eq. (2).[27] The standard equation[28–31] for the fracture toughness (K_{1c}) of a bar is:

$$K_{1c} = (3/2).(PLc^{1/2}).Y/(WD^2) = (2E\gamma_i)^{1/2} = (\sigma Y C^{1/2}) \quad (3)$$

$$Y = [A_0 + A_1(c/D) + A_2(c/D)^2 + A_3(c/D)^3 + A_4(c/D)^4] \quad (4)$$

where c is the notch depth, C is the critical crack length and Y is a dimensionless number, which is dependent on the geometry of the loading and the crack configuration with $L/D \approx 8$, $A_0 = +1.96$, $A_1 = -2.75$, $A_2 = +13.66$, $A_3 = -23.98$, $A_4 = +25.22$.[31] The fracture surface energy (γ_i) is a measure of the resistance to initiation of crack propagation. γ_i was calculated from Eq. (3), using experimental K_{1c} (by SENB) and Young's modulus values. Values for the work of fracture (γ_{WOF}) were calculated from load–deflection curves obtained from notched bars deformed in three-point bend, by measuring the area (U) under the load–deflection curve. γ_{WOF} is given by the following equation:[32,33]

$$\gamma_{WOF} = \{U/[2W(D-c)]\} \quad (5)$$

Grain sizes of polished and thermally etched (1500 °C, 10 min) surfaces were measured from photographs taken in the scanning electron microscope. Average grain size was determined from intercept measurements[34] on the observed plane, by using the standard Eq. (6):

$$\bar{D} = 1.56\bar{L} \quad (6)$$

where $\bar{D}$ is the average grain size and $\bar{L}$ is the average intercept length, taken over a large number of grains and measured on the plane of polish. All the values calculated for pure MgO and spinel composites were the average value of ~100 measurements of ~3 micrographs. Thermal shock parameter R''' was calculated from: $R''' = E/[\sigma_f^2.(1-\upsilon)]$, which gives information about available energy at fracture for resisting to crack propagation,[35–37] where υ is Poisson's ratio. The CamScan 4 SEM used in this study was equipped with an EDX system for elemental analysis. Secondary electron images (SEI) were used to examine the fracture surface, size, shape and texture of the particles; back scattered electron images (BEI), which provide atomic contrast, were used to indicate the presence and position of second phases in the polished surface of the multiphase materials.

3. Results and discussion

Calcination of MgO powder at 1300 °C for 2 h gave a mean particle size of ~0.4 μm using SEM and ~0.55 μm using BET. The average value of the calcined MgO powder was taken to be ~0.5 μm. The median particle sizes (d_{50}) of the Alcoa MR66 spinel, defined as 'A' (22 μm by using air classification), and the Britmag 67 spinel, defined as 'B' (24 μm by using a 150 μm sieve), are shown in Fig. 1(a) and (b). As shown in Fig. 2(a), Alcoa MR66 spinel particles (A) were regular in size and shape, because the use of air classification gave a narrow particle size distribution. However, Fig. 2(b) illustrated that there was a significantly broader distribution in the Britmag 67 spinel (B) particles; these consisted of agglomerated polycrystals, and which disintegrated during hot-pressing. Based on the above, it is suggested that powder agglomeration leads to inhomogeneous composites and variations in packing density, after hot-pressing. This statement implies that strength impairment as a result of microcracking does seem to be more severe in the spinel B composites containing the very large agglomerated particles of spinel.

Mechanical properties, critical crack length, MgO mean grain size, γ_i and γ_{WOF} values of MgO–spinel composites, which contain 22 μm MR66 (A) and 24 μm Britmag 67 spinel (B) particles, are given in Table 1.

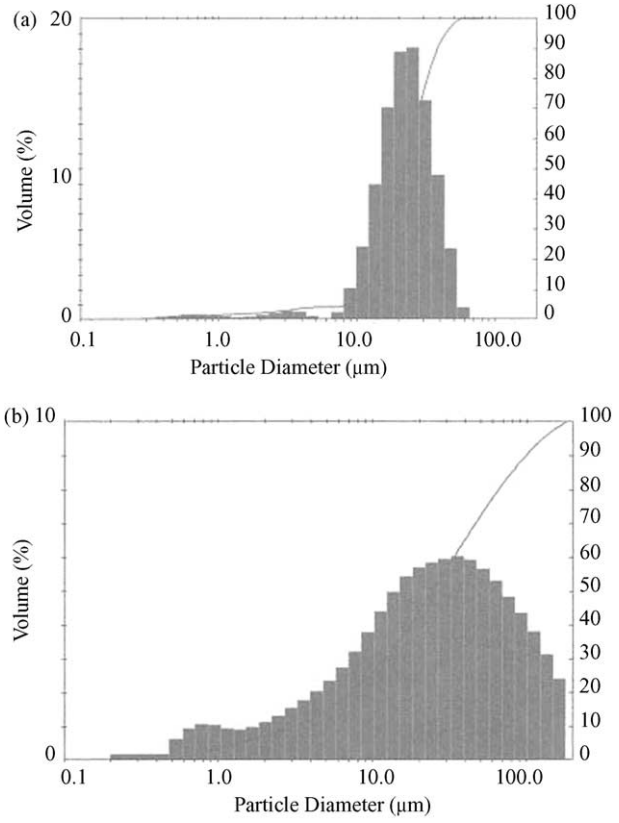

Fig. 1. Particle size distribution of (a) 22 μm spinel A and (b) 24 μm spinel B.

Composites obtained from spinel A and spinel B did not give the same strength values for similar loading, though the trends were similar. Composites prepared from the purer spinel A powder showed a more marked decrease in strength with increasing amounts of spinel. The addition of up to 10% of the less pure 24 μm spinel powder to MgO also decreased the strength significantly (~80%). Further additions caused no further loss (though there may have been a slight increase at 30% addition, but the scatter of data was larger). Spinel A type composites, for 10% addition, were approximately two times stronger than the spinel B type composites. This might be explained on the basis of the much narrower size distribution of the purer spinel A particles [Fig. 1(a)]. In contrast, spinel B particles were not homogeneously distributed in the microstructure, because of the effects of agglomeration, though a higher

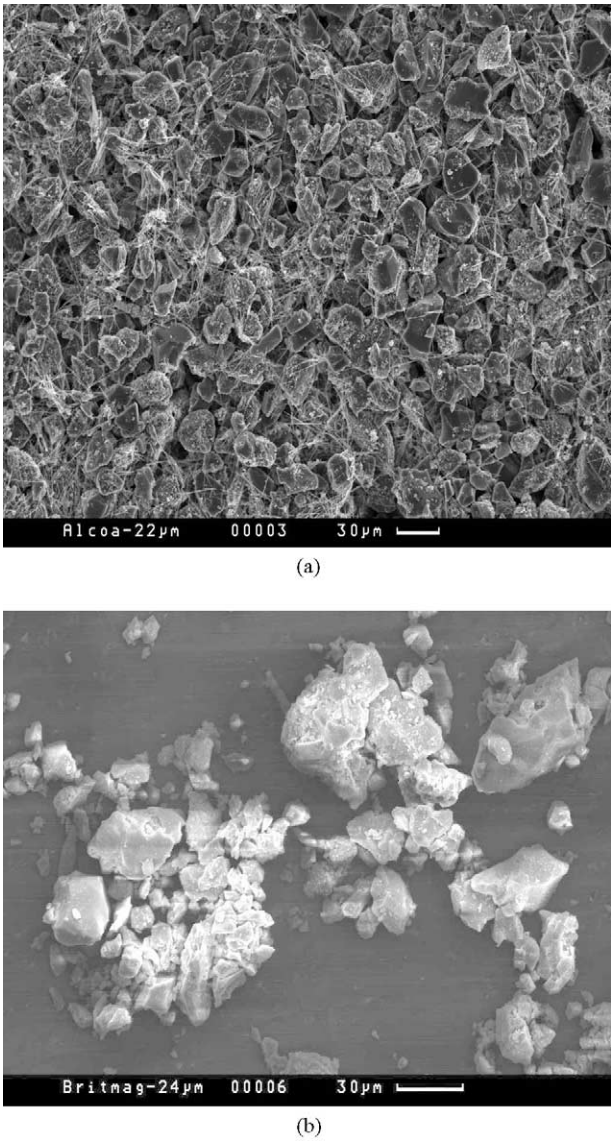

Fig. 2. SEM micrographs of (a) 22 μm Alcoa MR66 spinel powder (A) and (b) 24 μm Britmag 67 spinel powder (B).

Table 1
Mechanical properties and MgO grain size of spinel A and B composites[a]

	22 μm spinel (A) /%					24 μm spinel (B) /%				
	0	5	10	20	30	0	5	10	20	30
σ (MPa)	233±7	158±10	110±14	65±8	61±4	233±7	91±14	48±17	50±10	70±23
E (GPa)	268±30	215±42	152±38	111±20	80±5	268±30	200±11	136±18	136±15	76±4
K_{1c} (MPa m$^{1/2}$)	2.2±0.2	1.6±0.1	1.0±0.1	0.8±0.1	0.8±0.1	2.2±0.2	1.3±0.1	0.7±0.1	0.8±0.1	1.0±0.1
C (μm)	26±0.2	28±0.3	29±0.6	39±0.4	47±0.5	26±0.2	58±0.9	66±0.2	77±0.7	67±0.2
MgO grain size (μm)	32±2	70±7	87±3	50±6	41±5	32±2	64±4	58±6	52±9	45±3
γ_i (J m^{-2})	8.9±2.2	6.0±2.0	3.3±1.5	2.9±0.9	3.8±1.5	8.9±2.2	4.0±1.0	1.9±0.4	2.4±0.7	6.7±1.1
γ_{WOF} (J m^{-2})	39±5	64±8	61±4	64±3	68±6	39±5	54±5	57±2	59±3	64±7

[a] σ: strength, E: Young's modulus, K_{1c}: fracture toughness, C: critical crack length, γ_i: fracture surface energy, γ_{WOF}: work of fracture.

proportion of 50–100 μm particles disintegrated during hot-pressing. It is clear that spinel B composites, which contained of a large proportion of spinel particles of sizes much larger than the median sizes [Fig. 1(b)], therefore had increased microcracking (Fig. 4) and showed a more marked decrease in strength for 10% additions (Table 1), as compared to spinel A composites (Fig. 3). Agglomerated spinel particles resulted in longer interlinked transgranular and intergranular radial cracks (Fig. 4), because the hoop stress (at a given distance from the inclusion centre) is larger, the larger the inclusion size.

Composites prepared from spinel A powder in general showed a smaller amount of microcracking compared to composites obtained from spinel B particles (Figs. 3 and 4). This is assumed to be because spinel A particles had a much narrower in size distribution, while spinel B powder had a much broader particle size distribution, and extensive agglomeration. In composites containing low additions of spinel A particles (i.e. 5–10% 22 μm), there was a small amount of microcracking at grain boundaries (intergranular) radiating from spinel particles, but the cracks did not interlink. However, Fig. 3 shows that a large amount of longer cracks occurred with 20% additions, and cracks started linking. The higher the spinel content, the greater the crack length appeared to be. The spinel A particles were more homogeneously distributed mostly at the grain boundaries and some within the MgO grains, and there was no concentration of agglomerated spinel particles. This contrasts with materials containing spinel B particles, as seen in Fig. 4. Fig. 4 shows that interlinked transgranular and intergranular radial cracks in the MgO matrix appeared with the addition of 10% 24 μm spinel particles, and the crack length increased significantly. Groups of agglomerated spinel particles were linked by cracking in the MgO matrix. There was a marked broad distribution in agglomerated spinel particles, ranging ~10–24 μm, but groups of agglomerated spinel particles were varying up to approximately 90 μm. Furthermore, a large quantity of similar cracks was also observed in the agglomerated spinel particles with further addition of spinel B particles.

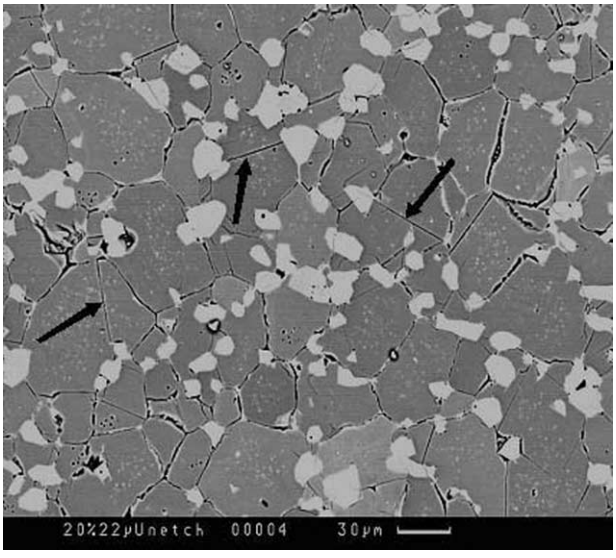

Fig. 3. SEM micrograph of a 20% 22 μm spinel A composite, showing crack length and linked microcracks between the spinel particles (dark grey: MgO, light grey: spinel).

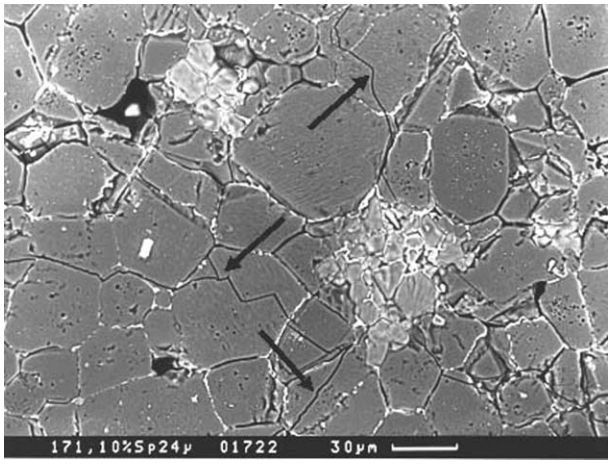

Fig. 4. SEM micrograph of a 10% 24 μm spinel B composite, showing crack length and linked microcracks between the spinel particles (dark grey: MgO, light grey: spinel).

The Young's modulus of spinel composites generally decreased with increasing spinel content (Table 1). There was little difference between the 22 and 24 μm spinel composites. The decrease in Young's modulus of spinel B composites was most significant, for up to 10% additions. At 10%, Young's modulus was approximately 50% of the value for pure MgO. Increasing the amount of spinel from 10 to 30%, had a relatively small effect. The loss of modulus can be explained in terms of radial crack propagation and ultimately interlinking. It appears that crack interlinking is completed at about 10% addition of spinel, undermining the mechanical integrity of the material, and changes little after this point.

Spinel content markedly affected the strength. There was a significantly greater decrease in strength for 24 μm compared to 22 μm spinel particles, and the 24 μm spinel particles were associated with formation of longer cracks than the 22 μm particles (Figs. 3 and 4). The total extent of cracking also increased with increasing concentration of spinel. The mean critical defect sizes (C) of the spinel A, and B, composites, calculated using Eqs. (3) and (4), increased approximately by factors of ~2 and 3 respectively, at maximum values, with increasing spinel content (Table 1). The calculated critical defect sizes of spinel A and B composites were the same order of magnitude as the actual crack lengths observed in the SEM. The particle size distribution of spinel B powder was much broader than that of spinel A, and this may have been responsible for the larger crack lengths seen in the SEM micrographs (Figs. 3 and 4). Spinel A powder had a narrower particle size distribution, which appeared to result in smaller maximum defect sizes. This indicates that the larger particle population determines the critical defect size. Table 1 also illustrates that accelerated grain growth occurred up to ~10% additions. With further additions of spinel (>10%), decelerated grain growth occurred, most probably because of the dominance of grain boundary pinning effects by the spinel grains. Both acceleration and deceleration were most marked for the 22 μm spinel particles, which were mostly located at the grain boundaries and partly within the grains.

It is suggested that spinel content and the composite crack size are more important factors determining the critical defect size than MgO grain size, in controlling strength through the Griffith relationship. In addition, particle interaction coupled with thermal expansion mismatch causing microcracking and interlinking, is the most important parameter.

Composites prepared from spinel A showed a general marked decrease in toughness with increasing spinel content. K_{1c} also decreased significantly with spinel B additions reaching a minimum for ~10%; however, further additions increased K_{1c} slightly. The general trend is for K_{1c} to decrease with spinel content. This trend is assumed to be in part a result of the observed decreasing Young's modulus, with an extending and interlinking microcrack network. This also indicates a decrease in fracture surface energy, because the amount of energy required to initiate crack propagation decreases with increasing concentration of pre-existing connecting cracks.

There was a general increase in γ_{WOF} with increasing spinel content (Table 1). Fracture surfaces of pure MgO showed a large proportion of transgranular cracks, with some intergranular cracks (Fig. 5). At low additions of spinel, transgranular cracks were still present with some intergranular cracks, in the fracture surfaces of each spinel composite. However, at higher additions of spinel ($\geqslant$10%), mostly intergranular fracture occurred (Fig. 6). It therefore appears that higher values of γ_{WOF} are associated with the occurrence of more intergranular fracture with increasing spinel additions.

The fracture of the magnesia-spinel composites is either semi-stable or stable, but never catastrophic, like MgO. It may be concluded that crack propagation is a much greater energy consuming process than crack initiation in these materials. For many industrial applications, the initiation of fracture is less important than γ_{WOF} and the degree of damage (e.g. further loss of mechanical integrity by strength and material loss through large scale fracture behind the hot face).[38] Large values of the γ_{WOF}/γ_i ratio were obtained in these composites (Fig. 7). This is a basic requirement for refractory materials to show good thermal shock damage resistance.[39] Fig. 7 illustrates that the 10% 24 μm spinel B composites showed the highest γ_{WOF}/γ_i ratio, by a factor of ~6, as compared to pure MgO. The 20% 22 μm spinel A composites also had ~5 times higher ratios than MgO. On the basis of the γ_{WOF}/γ_i

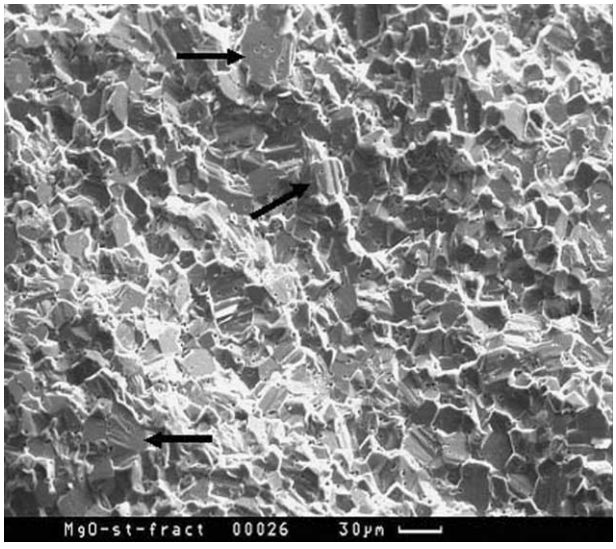

Fig. 5. Fracture surface of dense MgO, showing transgranular fracture.

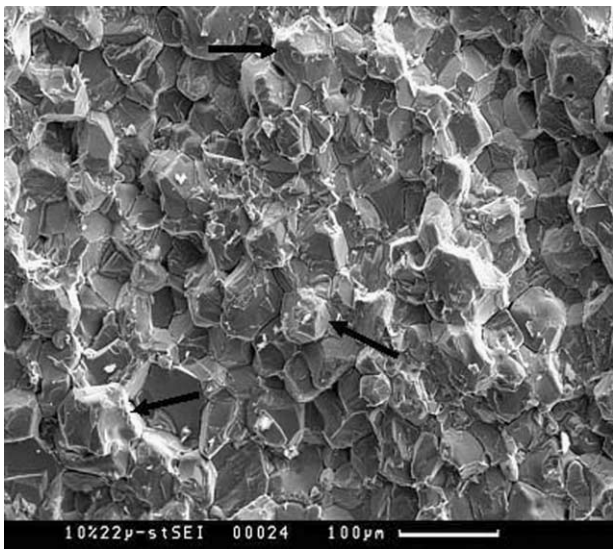

Fig. 6. Fracture surface of composite containing 10% 22 μm spinel A, showing intergranular fracture.

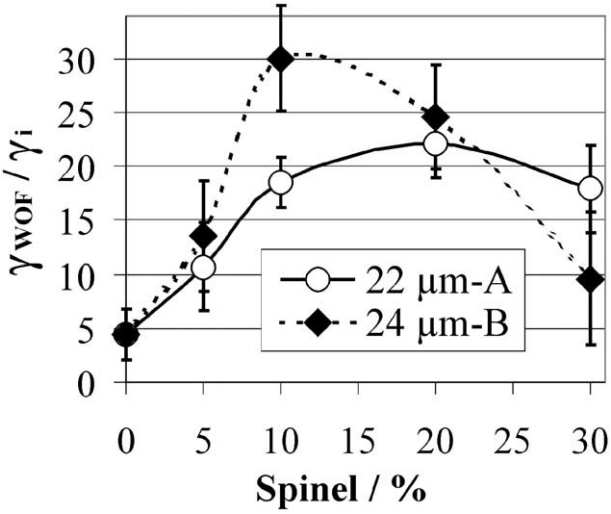

Fig. 7. γ_{WOF}/γ_i ratios, as a function of spinel A and B content.

ratio it might therefore have been expected that spinel B composites in general would show greater resistance to crack propagation, and to further thermal shock damage than spinel A composites (Fig. 7).

Fig. 8 shows that the R''' parameter increased with all spinel additions in comparison with pure MgO. The thermal shock resistance for a given spinel A and B content, in terms of the R''' parameter, would therefore be predicted to be 5 and 12 times (20% 22 μm and 10% 24 μm) better than that of pure MgO. Composites containing the 24 μm spinel stand out as having significantly higher R''' values. This may be because the decline in strength with increasing spinel content is now much greater than the corresponding decrease in Young's modulus (Table 1). It would be predicted on this basis that 24 μm spinel B would provide a significant improvement in resistance to thermal shock damage through increased difficulty of crack propagation, with a maximum at ~10% spinel addition. This is assumed to be the cause of the increased microcracking compared to that in type A spinel materials. This shows that the marked detrimental effect of the larger size distribution spinel B particles on strength should in theory provide the greatest benefit for thermal shock resistance.

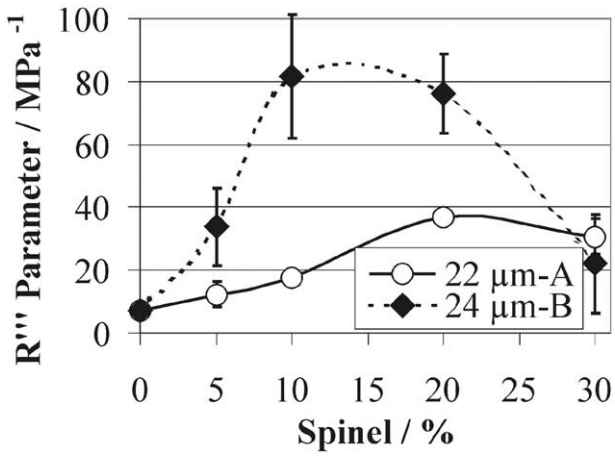

Fig. 8. R''' parameter as a function of spinel A and B content.

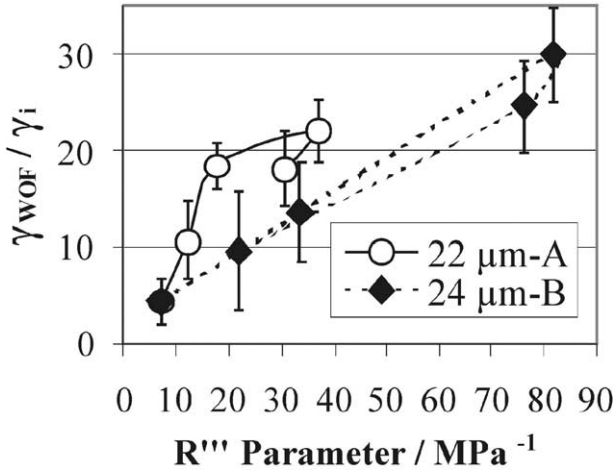

Fig. 9. γ_{WOF}/γ_i ratios depending on spinel A and B content, as a function of R''' parameter.

After thermal shock parameter, R''', was calculated, these predictions were compared with the experimentally found γ_{WOF}/γ_i ratios in order to predict thermal shock behaviour of those materials. Fig. 9 shows that γ_{WOF}/γ_i ratios approximately gave similar results with respect to R''' parameter, which were in good agreement with each other. Spinel A particles resulted in shorter initial crack propagation distances from the spinel particles (Fig. 3); however, spinel B particles with increasing amount of spinel were the origins of longer cracks, which were linked (Fig. 4). It might therefore have been expected that the thermal shock resistance of 10% 24 μm spinel B composites, resulting from resistance to

microcrack propagation and interlinking, was predicted to be approximately 2 times greater than those obtained from 20% 22 μm spinel A (Fig. 8). This prediction was confirmed by the γ_{WOF}/γ_i ratio for these MgO–spinel composites, which suggested an optimum composition of 10% 24 μm spinel B particles (Fig. 7). On the basis of γ_{WOF}/γ_i ratios and the calculated R''' values, spinel B particles appear to be generally more beneficial than spinel A particles (Fig. 9), for which a very much larger volume appears to be required to achieve a similar improvement (Fig. 7).

4. Conclusions

Strength, Young's modulus, fracture toughness and fracture surface energy values of composites in general decreased markedly with increasing spinel content in comparison with MgO. It is therefore clear that the development of thermal shock resistance in the magnesia–spinel composites cannot be linked to any increased fracture toughness. Materials containing 22 μm spinel had short length cracks originating from the spinel particles; the 24 μm spinel B particles were the origin of longer cracks, and more crack initiation sites. This is likely to have been because the spinel B contained a high proportion of much coarser particles than the mean, indicating particle interaction, because of its broad particle size distribution, and it caused much longer microcracks and more crack interlinking, compared to spinel A. The calculated critical defect sizes, and also actual crack lengths, increased with spinel additions. MgO grain size varied with spinel content but this appeared to have little if any influence on strength. It is clear that the critical defect size is not significantly associated with the MgO grain size, but with the thermal expansion mismatch, causing microcracking, longer interlinked cracks, spinel particle size distribution and content, and which are likely to be the major factors determining mechanical properties.

The improvement in thermal shock resistance predicted by the R''' parameter, and observed experimentally from the γ_{WOF}/γ_i ratios, was explained by the large decreases in strength, and the lesser decreases in Young's modulus. The change in the fracture path from transgranular to intergranular fracture with spinel additions resulted in an increase in the areas under the load–displacement curve, which indicated marked crack interlinking with the higher γ_{WOF} values, requiring more energy for the fracture process. The improved resistance to thermal shock in magnesia–spinel composites can therefore be attributed to the microcrack networks developed around the spinel particles. It might therefore have been expected that resistance to crack propagation in general would be greater with materials containing spinel B particles. On this basis it would be predicted that further deterioration in strength of the composites as a result of thermal shock would be a minimum for 10–20% of the 24 μm spinel B powder. The 22 μm spinel A powder was ranked second, at 20–30% spinel additions.

Acknowledgements

Lafarge (UK) and Alcoa International (UK) Ltd. are thanked for supplies of materials. The contributions of Dr. P.D. Warren, Prof. B. Rand and the late Prof. R.W. Davidge are gratefully acknowledged. P. Bartha, S. Plint, and M.W. Roberts are also thanked for helpful discussions. This work was in part carried out as part of a PhD programme in the Department of Materials of the University of Leeds, and the authors thank the Technical Staff of the Department for their assistance. Financial support was provided in part by the Council of Higher Education in Turkey.

References

1. Rigby, G. R., The spinels and their relation to chrome ores. In *Ceramics: A Symposium*, ed. A. T. Green and G. H. Stewart. The British Ceramic Society, Stoke-on-Trent, 1953, pp. 488–512.
2. Chesters, J. H., *Refractories, Production and Properties*. The Iron and Steel Institute, London, 1973.
3. Reyes Sanchez, J. A. and Toledo, O. D., New developments of magnesite-chrome brick and magnesite-spinel for cement rotary kilns higher thermal shock resistance and higher coating adherence. In *UNITECR 89*, Anaheim, USA, 1989, pp. 968–979.
4. Eusner, G. R. and Hubble, D. H., Technology of spinel-bonded periclase brick. *J. Am. Ceram. Soc.*, 1960, **43**, 292–296.
5. Bray, D. J., Toxicity of chromium compounds formed in refractories. *Bull. Amer. Ceram. Soc.*, 1985, **64**, 1012–1016.
6. Cooper, S. C. and Hodson, P. T. A., Magnesia-magnesium aluminate spinel as a refractory. *Trans. J. Br. Ceram. Soc.*, 1982, **81**, 121.
7. Dal Maschio, R., Fabbri, B. and Fiori, C., Industrial applications of refractories containing magnesium aluminate spinel. *Industrial Ceramics*, 1988, **8**, 121–126.
8. Tokunaga, K., Kozuka, H., Honda, T. and Tanemura, F., Further improvements in high temperature strength, coating adherence, and corrosion resistance of magnesia-spinel bricks for rotary cement kiln. In *UNITECR '91*, Aachen, Germany, 1991, pp. 431–435.
9. Soady, J. S. and Plint, S., A quantitative thermal shock approach to the development of magnesia-spinel refractories for the cement kiln. In *UNITECR '91*, Aachen, Germany, 1991, pp. 443–449.
10. Tabbert, W. and Klischat, H. J., Magnesia spinel bricks for the cement industry. In *Proceedings Beijing China Symposium*, China, 1992, pp. 424–430.
11. Aksel, C., Rand, B., Riley, F. L. and Warren, P. D., Mechanical properties of magnesia-spinel composites. *J. Eur. Ceram. Soc.*, 2002, **22**, 745–754.
12. Aksel, C. and Warren, P. D., Thermal shock parameters [R, R''' and R''''] of magnesia–spinel composites. *J. Eur. Ceram. Soc.*, 2003, **23**, 301–308.
13. Shackelford, J. F., Alexander, W. and Park, J. S., (eds), *CRC Materials Science and Engineering Handbook*. CRC Press, Boca Raton, FL, 1994.

14. Burnett, S. J., *Properties of Refractory Materials*. UKAEA Research Group Report, Harwell, 1969.
15. Aksel, C., *Thermal Shock Behaviour and Mechanical Properties of Magnesia–Spinel Composites*. PhD Thesis, Department of Materials Engineering, University of Leeds, Leeds, UK, 1998.
16. Evans, A. G., Perspective on the development of high toughness ceramics. *J. Am. Ceram. Soc.*, 1990, **73**, 187–206.
17. Matelaro, V. R. and Zanotto, E. D., Residual stresses in soda-lime–silica glass ceramic. *J. Non-Crystalline Solids*, 1996, **194**, 297–304.
18. Henderson, R. J. and Chandler, H. W., The nonlinear mechanical behaviour of high performance refractories. In *Euro Ceramics V, Part 1, Extended Abstracts of the 5th Conference and Exhibition of the European Ceramic Society, Vols. 132–136, Key Engineering Materials*, Versailles, France, 1997, pp. 504–507.
19. Klischat, H. J. and Bartha, P., Further development of magnesia spinel bricks with their own specific properties for lining the transition and sintering zones of rotary cement kilns. *World Cement, 1992, 52–58*.
20. Aksel, C., Davidge, R. W., Warren, P. D. and Riley, F. L., Investigation of thermal shock resistance in model magnesia-spinel refractory materials. In *IV. Ceramic Congress, Proceedings Book, Part 1*, Eskisehir, Turkey, 1998, pp. 193–199.
21. Aksel, C., Davidge, R. W., Warren, P. D. and Riley, F. L., Mechanical properties of model magnesia-spinel composite materials. In *Euro Ceramics V, Part 3, Extended Abstracts of the 5th Conference and Exhibition of the European Ceramic Society, Vols. 132–136, Key Engineering Materials*, Versailles, France, 1997, pp. 1774–1777.
22. Aksel, C., Davidge, R. W., Knott, P. and Riley, F. L., Mechanical properties of magnesia–magnesium aluminate spinel composites. In *III. Ceramic Congress Proceedings Book, Vol. 2, Engineering Ceramics*, Istanbul, Turkey, 1996, pp. 172–179.
23. British Standard Testing of Engineering Ceramics. *BS 7134 Section 1.2*, 1989.
24. Davidge, R. W., *Mechanical Behaviour of Ceramics*. Cambridge University Press, Cambridge, 1979.
25. Rice, R. W., Strength and fracture of hot-pressed MgO. *Proc. Brit. Ceram. Soc.*, 1972, **20**, 329–363.
26. ASTM C1161-90, *Standard Test Method for Flexural Strength of Advanced Ceramics at Ambient Temperature, Annual Book of ASTM Standards*, Vol. 15.01. ASTM, 1991, pp. 327–333.
27. ASTM D790M-86, *Standard Test Methods for Flexural Properties of Unreinforced and Reinforced Plastics and Electrical Insulating Materials, Annual book of ASTM Standards*, Vol. 08.01. ASTM, 1988, pp. 290–298.
28. Larson, D. R., Coppola, J. A., Hasselman, D. P. H. and Bradt, R. C., Fracture toughness and spalling behaviour of high-Al_2O_3 refractories. *J. Am. Ceram. Soc.*, 1974, **57**, 417–421.
29. ASTM E399-90, *Standard Test Method for Plane-Strain Fracture Toughness of Metallic Materials, Annual Book of ASTM Standards*, Vol. 03.01. ASTM, 1991, pp. 485–515.
30. ASTM D5045-91, *Standard Test Methods for Plane-Strain Fracture Toughness and Strain Energy Release Rate of Plastic Materials, Annual Book of ASTM Standards*, Vol. 08.03. ASTM, 1991, pp. 728–736.
31. Brown, W. F. and Srawley, J. E., *Plane Strain Crack Toughness Testing of High Strength Metallic Materials*. ASTM Special Technical Publication No. 410, 1967.
32. Davidge, R. W. and Tappin, G., The effective surface energy of brittle materials. *J. Mater. Sci.*, 1967, **3**, 165–173.
33. Coppola, J. A., Hasselman, D. P. H. and Bradt, R. C., On the measurement of the work-of-fracture of refractories. *Am. Ceram. Soc. Bull.*, 1972, **17**, 578.
34. Mendelson, M. I., Average grain size in polycrystalline ceramics. *J. Am. Ceram. Soc.*, 1969, **52**, 443–446.
35. Hasselman, D. P. H., Elastic energy at fracture and surface energy as design criteria for thermal shock. *J. Am. Ceram. Soc.*, 1963, **46**, 535–540.
36. Hasselman, D. P. H., Unified theory of thermal shock fracture initiation and crack propagation in brittle ceramics. *J. Am. Ceram. Soc.*, 1969, **52**, 600–604.
37. Sack, R. A., Extension of Griffith's theory of rupture to three dimensions. In *Proc. Physical Soc.*, Vol. 58. London, 1946, pp. 729–736.
38. Hasselman, D. P. H., Strength behaviour of polycrystalline alumina subjected to thermal shock. *J. Am. Ceram. Soc.*, 1970, **53**, 490–495.
39. Nakayama, J., Abe, H. and Bradt, R. C., Crack stability in the work-of-fracture test: refractories applications. *J. Am. Ceram. Soc.*, 1981, **64**, 671–675.